Three-dimensional Baxter-Wu model

L. N. Jorge*
Instituto Federal do Mato Grosso, Campus Cáceres, CEP. 78200-000, Cáceres, Mato Grosso, Brazil

L. S. Ferreira† and A. A. Caparica‡
Instituto de Física, Universidade Federal de Goiás, Av. Esperança s/n, 74.690-900, Goiânia, GO, Brazil

(Received 18 August 2018; revised manuscript received 28 March 2019; published 27 September 2019)

A classic three-dimensional spin model, based upon the Baxter-Wu scheme, is presented. It is found, by entropic sampling simulations, that the behavior of the energy and magnetization fourth-order cumulants points to a first-order phase transition. A finite-size procedure was performed, confirming that the system scales with the dimensionality $d = 3$, yielding a high-resolution estimate of the transition temperature as $T_c = 11.377485(29)$.

DOI: 10.1103/PhysRevE.100.032141

I. INTRODUCTION

The study of three-dimensional (3D) spin models in statistical physics has great importance in materials science, since it can describe, predict, or even design real systems. We can cite the well-known Ising model that is used to describe the Fe-Al magnetic alloy [1–3], once it is arranged in a bcc structure composed of two interpenetrating cubic lattices. For the disordered case, the phase diagram has been described using the site-diluted spin-1 Blume-Capel model in a simple cubic arrangement via a mean-field renormalization group approach in the pair approximation [4]. Such a technique and model were also used to characterize Fe-Ni-Mn and Fe-Al-Mn alloys [5]. The Ising model is also used to construct metamagnets in thin film geometry models. These systems were studied via Wang-Landau procedure and by importance sampling Monte Carlo (MC) simulations in investigations of their equilibrium phase diagram [6]. Such a model was extended to the understanding of nonequilibrium relaxation processes in Co-Cr superlattices [7]. Metamagnetic compounds $FeCl_2$ and $FeBr_2$ have had their properties simulated by a study of a 3D spatially anisotropic Ising superantiferromagnet in the presence of a magnetic field [8], where a rich phase diagram was constructed. There are in nature hexagonal arrangements, such as some magnetic systems. Based on MC simulations, Ma *et al.* have presented results of a film model that is described by a 3D layered honeycomb lattice [9]. This kind of lattice was used by Wang *et al.* in the characterization of molecular-based magnetic film $AFe^{II}Fe^{III}(C_2O_4)_3$ [10]. Most of the hexagonal magnetic materials are described via the Ising model in a triangular lattice, as is the case of $Ca_3CO_2O_6$, where the steplike magnetization behavior is strongly dependent on the external field and temperature [11–13]. Hexagonal nanoparticles and nanowires with a core-shell structure, like CuS-Cu_2S with mixed spin $(1/2; 1)$ and spin-1 Zn-Se, have been successfully predicted and synthesized [14–20].

Although there are so many models in hexagonal arrangements in nature or predicted in literature, a 3D model via Baxter-Wu interactions is lacking. Therefore the present work aims at modeling a 3D system that obeys a three-spin interaction like in the two-dimensional (2D) Baxter-Wu model, and investigating the order of the phase transition and estimating the subsequent thermodynamic properties, using entropic sampling simulations.

II. THE 3D BAXTER-WU MODEL

Proposed by Wood and Griffiths [21] in 1972 and exactly solved by Baxter and Wu [22–24], the Baxter-Wu model is a spin model that considers terms of triple coupling between the spins. It consists in a magnetic system defined on a 2D triangular lattice, where, for the spin-1/2 case, the spins variables can assume the values $s_i = \pm 1$ and are located at the vertices of the triangles. The three-spin interaction is governed by the Hamiltonian

$$H_{\mathrm{BW}} = -J \sum_{\langle i,j,k \rangle} s_i s_j s_k, \tag{1}$$

where J is the nearest-neighbor coupling parameter between the spins that fixes the energy scale, and the sum extends over all triangular faces of the lattice.

To construct the 3D version of the Baxter-Wu model, we consider a regular hexagon on the horizontal plane, with six spins in the vertices. In its center, there are three axes crossing it, in such a way that each one can be associated to a hexagon forming an angle of 60° with the initial plane, as shown in Fig. 1(a). In this figure we see that the initial hexagon is formed by the dots (1,2,3,4,5,6), and in its center is the zero site. The other three hexagons are formed by (1,9,8,4,12,10), (2,9,7,5,12,11), and (3,8,7,6,10,11). So a spin, that in the 2D case has six nearest neighbors and is surrounded by six triangular faces, has in this case 12 nearest neighbors and counts 24 triangular faces surrounding it.

In this scheme, the three sites that belong to the upper plane, are located above the center of three alternated triangular faces, while the other three in the lower plane are located

*lucasnjorge@gmail.com
†lucas.if.ufg@gmail.com
‡caparica@ufg.br

 ©2019 American Physical Society

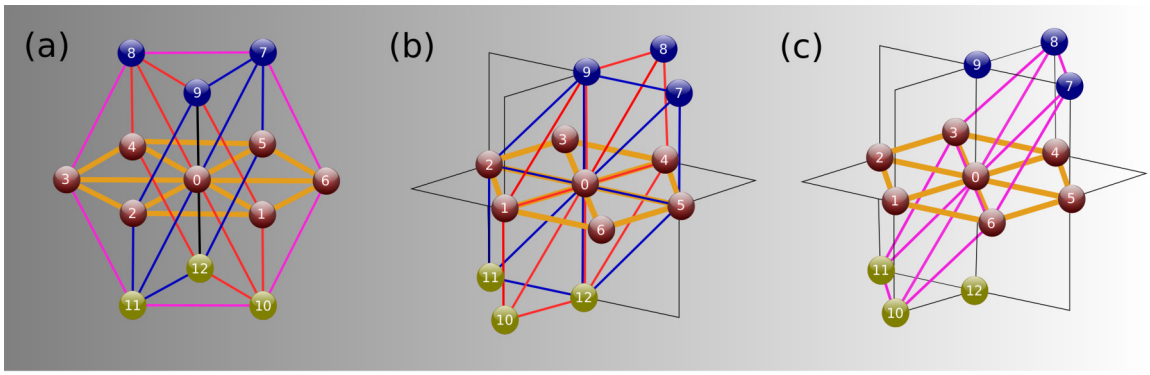

FIG. 1. (a) Three-dimensional lattice of the Baxter-Wu model. (b) Three-dimensional lattice of the Baxter-Wu model transposed into a cubic lattice. (c) The oblique plane.

below the centers of the other three triangular faces, as shown in Fig. 1(a). This lattice is known as a face-centered cubic (fcc) [25].

Therefore, the 3D Baxter-Wu model is defined in a 3D lattice with triangular interactions, with the energy given by

$$H_{\mathrm{BW3D}} = -J \sum_{\langle i,j,k \rangle} s_i s_j s_k, \tag{2}$$

where the sum extends over all possible triangular faces of the lattice and the spin variables are located at the vertices of the triangles and can assume the integer values $s_i = \pm 1$. J is the constant that scales the energy of the lattice, being the same in all directions. Unlike the 2D version of the model, which displays four ground-state configurations—one ferromagnetic and three ferrimagnetic—the 3D Baxter-Wu model has a single ground-state configuration, namely, the ferromagnetic one. When we try to construct a 3D ferrimagnetic configuration, the triangular faces are satisfied for two planes, but for the third and fourth planes, frustrations appear, showing that it is impossible to obtain such ferrimagnetic constructions in three dimensions with the ground-state energy. Notwithstanding one can stack up ferrimagnetic planes constructing an ordered configuration, but its energy will be higher than that of the ground state due to the frustrations in the triangular faces between the planes. The minimum energy of such a construction will occur when one follows the sequence a, b, c, a, b, c,..., where a, b, and c are each one of the three 2D ferrimagnetic ground-state configurations.

The configurations on the structure described above may be transposed to isomorphic configurations on a cubic lattice as shown in Figs. 1(b) and 1(c), where we see that three hexagons lie on the Cartesian planes, and the last one lies on a oblique plane. The Hamiltonian may then be decomposed in sums over four planes:

$$H = -J\left[\sum_{\langle i,j,k \rangle} s_i s_j s_k\right]_{XY}, \quad -J\left[\sum_{\langle i,j,k \rangle} s_i s_j s_k\right]_{XZ}, \quad -J\left[\sum_{\langle i,j,k \rangle} s_i s_j s_k\right]_{YZ}, \quad -J\left[\sum_{\langle i,j,k \rangle} s_i s_j s_k\right]_{\mathrm{Obl.}}, \tag{3}$$

which extend over all triangles of the lattice in each plane XY, XZ, YZ [Fig. 1(b)], and the oblique plane [Fig. 1(c)], respectively.

In the cubic scheme, the energy of a particular configuration is given by (see Fig. 2)

$$\begin{aligned} E = \frac{J}{3}\Bigg[& \sum_{i=1}^{L}\sum_{j=1}^{L}\sum_{k=1}^{L} s_{i,j,k}(s_{i+1,j,k}s_{i,j-1,k}+s_{i,j-1,k}s_{i-1,j-1,k}+s_{i-1,j-1,k}s_{i-1,j,k} + s_{i-1,j,k}s_{i,j+1,k}+s_{i,j+1,k}s_{i+1,j+1,k}+s_{i+1,j+1,k}s_{i+1,j,k}) \\ & + \sum_{i=1}^{L}\sum_{j=1}^{L}\sum_{k=1}^{L} s_{i,j,k}(s_{i+1,j,k}s_{i,j,k+1}+s_{i,j,k+1}s_{i-1,j,k+1}+s_{i-1,j,k+1}s_{i-1,j,k} + s_{i-1,j,k}s_{i,j,k-1} + s_{i,j,k-1}s_{i+1,j,k-1}+s_{i+1,j,k-1}s_{i+1,j,k}) \\ & + \sum_{i=1}^{L}\sum_{j=1}^{L}\sum_{k=1}^{L} s_{i,j,k}(s_{i,j,k+1}s_{i,j-1,k}+s_{i,j-1,k}s_{i,j-1,k-1}+s_{i,j-1,k-1}s_{i,j,k-1} + s_{i,j,k-1}s_{i,j+1,k} + s_{i,j+1,k}s_{i,j+1,k+1}+s_{i,j+1,k+1}s_{i,j,k+1}) \\ & + \sum_{i=1}^{L}\sum_{j=1}^{L}\sum_{k=1}^{L} s_{i,j,k}(s_{i-1,j-1,k}s_{i-1,j,k+1} + s_{i-1,j,k+1}s_{i,j+1,k+1} + s_{i,j+1,k+1}s_{i+1,j+1,k} + s_{i+1,j+1,k}s_{i+1,j,k-1} + s_{i+1,j,k-1}s_{i,j-1,k-1} \\ & + s_{i,j-1,k-1}s_{i-1,j-1,k})\Bigg], \end{aligned}$$

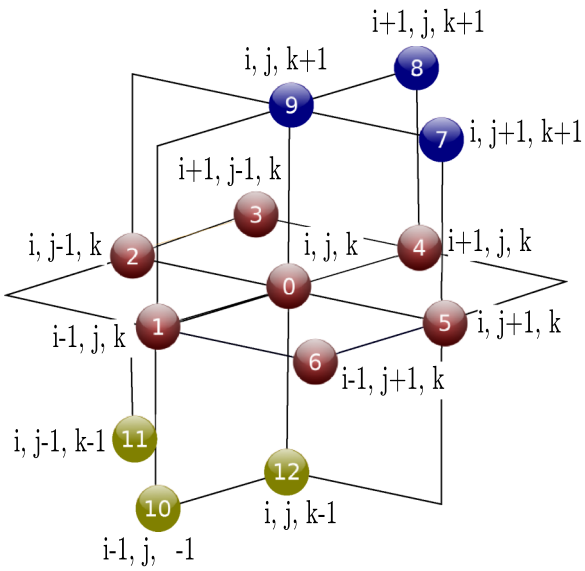

FIG. 2. Indexed spins with the spin i, j, k in the center for guiding the understanding of the Hamiltonian in the cubic lattice.

where the division by three is because in this sum each triangular face is counted three times.

In this work we adopted the order parameter as the total magnetization of the system, $M = \sum_{i,j,k=1}^{L} s_{i,j,k}$ [26–28]; thus, in the simulations we picked only nonmultiples of three lattice sizes.

III. ENTROPIC SAMPLING SIMULATIONS

The entropic simulations applied to our model are based on the Wang-Landau method [29], which by means of a random walk in energy space allows the construction of the density of states $g(E)$, generating a flat histogram for the energy distribution, and then the estimation of the canonical averages of any thermodynamic quantities. In our simulations we include some improvements that enhance the accuracy and lead to substantial savings in CPU time. Namely, (1) we adopt the Monte Carlo sweep before updating the density of states, avoiding taking into account highly correlated configurations, (2) we begin to accumulate the microcanonical averages only from the eighth Wang-Landau level (f_7), such that we discard the initial configurations that do not match with those of maximum entropy [30], (3) we use a checking parameter ε for halting the simulation [31] (the computational process is halted if the integral of the specific heat over a range of temperature calculated with the current density of states during the simulations varies less then 10^{-4} during a whole Wang-Landau level), and (4) we begin all simulations, for all lattice sizes, beginning from the outputs of a single run up to the Wang-Landau level f_6, because up to this point the current density of states is not biased yet and can proceed to any final result that would be obtained beginning from the first Wang-Landau level f_0 [32], a procedure that allows saving about 60% of CPU time.

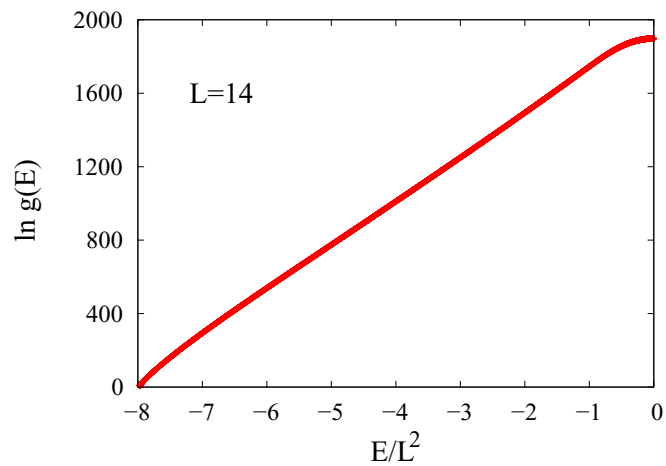

FIG. 3. Logarithm of the density of states for the $L = 14$ lattice.

IV. RESULTS

We carried out entropic simulations for $L \times L \times L$ lattices, picking $L = 8$, 10, 14, 16, and 20, with 24, 20, 20, 16, and 16 independent runs, respectively. In Fig. 3 we show the logarithm of the density of states of the lattice size $L = 14$.

The behavior of the fourth-order energy and magnetization cumulants

$$U_X(L) = 1 - \frac{\langle X^4 \rangle}{3\langle X^2 \rangle^2}, \quad X \equiv E, M \tag{4}$$

shown in Figs. 4 and 5 give us solid evidence that our model undergoes a first-order phase transition. The energy cumulants intersect at a point close to the transition temperature, while the magnetization cumulants exhibit sharp negative minima, as expected in a discontinuous phase transition. In addition, the energy probability distribution

$$P(E, T) = g(E)e^{-\frac{E}{k_B T}} \tag{5}$$

displays double peaks with a null probability valley between them, as we see in Fig. 6. Usually these peaks are symmetric, and then it is common to determine the transition temperature

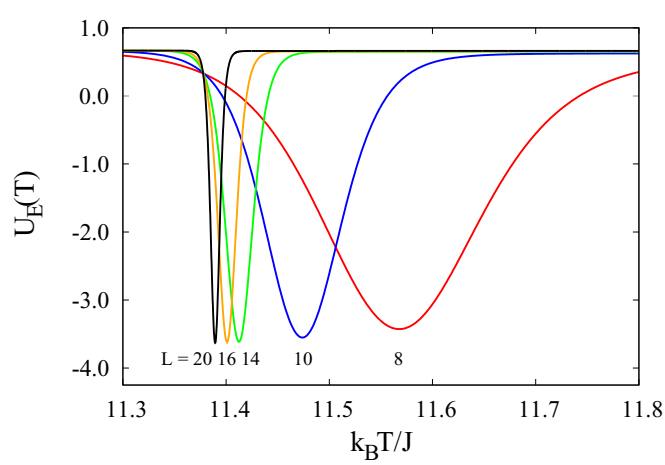

FIG. 4. Fourth-order energy cumulants as functions of temperature.

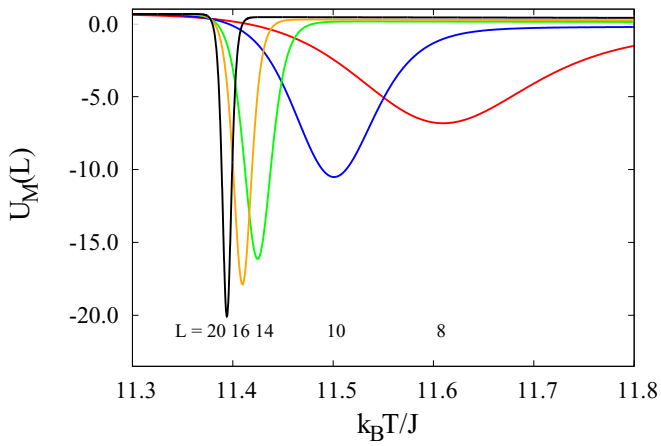

FIG. 5. Fourth-order magnetization cumulants as functions of temperature.

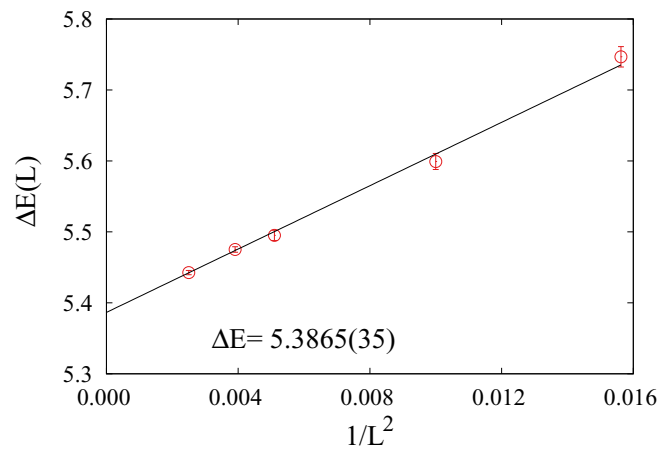

FIG. 7. Energy variation between the peaks of energy probability against $1/L^2$.

as that when the peaks reach the same hight. Nonetheless in our case they are asymmetric, and we find the transition temperature as that of the same weight, that is, when the areas below the maxima are the same [33].

A quantity which is intrinsically related to a first-order phase transition is the latent heat, which can be measured as the difference of the energies of the two peaks in the energy probability distribution and scales with L^{d-1} [34,35]. In Fig. 7 we show the finite-size scaling behavior yielding $\Delta E = 5.3865(35)$.

In a system that suffers a discontinuous phase transition it is expected that the maxima of the specific heat and the susceptibility should scale with the dimensionality. Another quantity that displays the dimensionality of the system in a discontinuous phase transition is $1/\nu$ in [26,36–38]

$$V_j \approx \frac{1}{\nu} \ln L + \mathcal{V}_j(tL^{\frac{1}{\nu}}). \tag{6}$$

In Fig. 8 we present the finite-size scaling behavior of these quantities, yielding $d_{C_v} = 2.9812(46)$, $d_\chi = 3.016(12)$, and $d_{V_j} = 3.0148(23)$. In order to get our final result for d, the dimensionality, we take an average of these values with unequal error bars, obtaining $d_{C_v,\chi,V_j} = 3.0083(20)$.

According to Fisher and Berker [34], in first-order transitions all finite-size scaling procedures are made in terms of powers of the lattice size, L^{-d}. Once confirmed that the system scales with the dimensionality, we can proceed with the determination of the transition temperature as the extrapolation for $L \to \infty$ ($L^{-d} = 0$) of the best linear fits of the temperatures of the maxima of the specific heat and the susceptibility, the minima of the energy and magnetization fourth-order cumulants, and the temperatures where the energy probability distribution displays double peaks of the same weight. In Fig. 9 we depict these best fits of these quantities for our simulations. The final estimate for the transition temperature was taken as the mean with unequal error bars of the five values obtained from fits for each thermodynamic function and was $T_c = 11.377485(29)$.

Many years after the publication of the 2D Baxter-Wu model, a system of adsorbed atoms or molecules in single

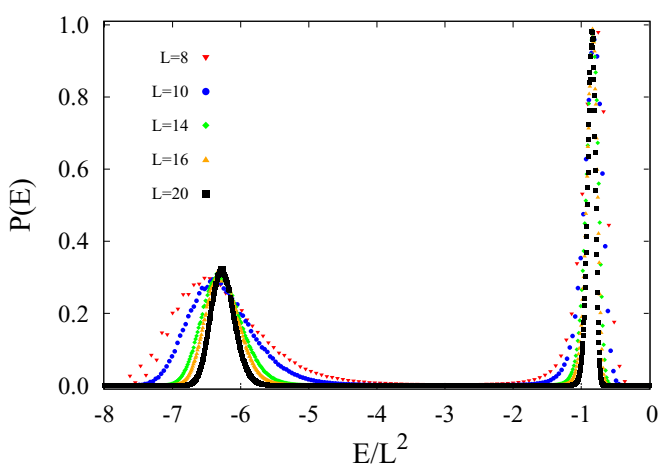

FIG. 6. Energy probability distributions as functions of the energy per particle at the temperatures where the areas below the maxima are the same.

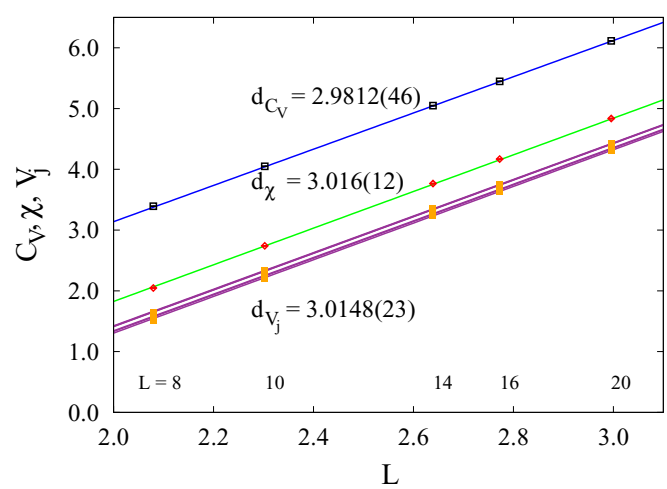

FIG. 8. Log-log plot of the maxima of the specific heat, susceptibility, and cumulants V_j with lattice size. The linear coefficients are close to the dimensionality of the system. The error bars are less than the symbols.

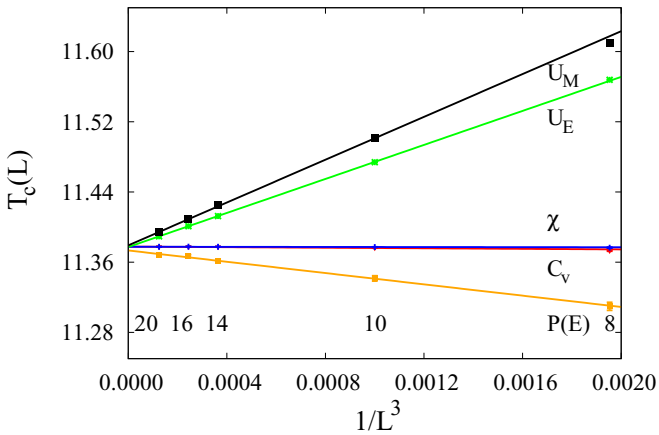

FIG. 9. Dependence on temperature of the minima of the energy and magnetization cumulants, maxima of specific heat and susceptibility, and double peaks of the same weight of energy density of probability, against $1/L^3$.The error bars are less than the symbols.

crystals and their universality class has been experimentally determined. We can site the compounds chemisorbed overlayer p(2 × 2) oxygen on Ni(111) [39], the adsorption system O-Ru(0001) [40] at the 1/4 monolayer, and the (2 × 2)-2H structure on Ni(111) [41]. They are 2D triangular systems that belong to same universality class of the 2D Baxter-Wu model. In the work of Barkema *et al.* [42], they have studied the Cu adsorbed on a Cu (111) surface. They considered an Ising model in a triangular lattice and, in addition to the nearest-neighbor spins interactions, they have taken into account triple interactions as in the Baxter-Wu model. We hope this 3D model may also consist of an useful platform for the simulation of existing compounds in nature.

V. CONCLUSIONS

In this work we proposed a 3D model inspired by the 2D Baxter-Wu model. The structure of the model corresponds to a FCC lattice. We studied its properties through extensive entropic sampling simulations and found that the system undergoes a first-order order-disorder transition, since the thermodynamic properties scale with the dimensionality of the system $d = 3$. We also carried out a high-precision estimation of the transition temperature and the latent heat.

ACKNOWLEDGMENTS

We acknowledge the computer resources provided by LCC-UFG and IF-UFMT. L.N.J. and L.S.F. acknowledge the support by FAPEG and CAPES, respectively.

[1] D. Dias, J. R. de Sousa, and J. Plascak, Phys. Lett. A **373**, 3513 (2009).
[2] J. A. Plascak, L. E. Zamora, and G. A. Pérez Alcazar, Phys. Rev. B **61**, 3188 (2000).
[3] A. Freitas, D. de Albuquerque, and N. Moreno, Physica A (Amsterdam) **391**, 6332 (2012).
[4] D. Dias and J. Plascak, Phys. Lett. A **375**, 2089 (2011).
[5] D. Peña Lara, G. A. Pérez Alcázar, L. E. Zamora, and J. A. Plascak, Phys. Rev. B **80**, 014427 (2009).
[6] Y.-L. Chou and M. Pleimling, Phys. Rev. B **84**, 134422 (2011).
[7] T. Mukherjee, M. Pleimling, and C. Binek, Phys. Rev. B **82**, 134425 (2010).
[8] O. D. Salmon, M. A. Neto, J. R. Viana, I. T. Padilha, and J. R. de Sousa, Phys. Lett. A **377**, 1991 (2013).
[9] B. Ma and W. Jiang, IEEE Trans. Magn. **47**, 3118 (2011).
[10] W. Wang, W. Jiang, D. Lv, and F. Zhang, J. Phys. D **45**, 475002 (2012).
[11] A. Maignan, V. Hardy, S. Hebert, M. Drillon, M. R. Lees, O. Petrenko, D. M. K. Paul, and D. Khomskii, J. Mater. Chem. **14**, 1231 (2004).
[12] A. Maignan, C. Michel, A. Masset, C. Martin, and B. Raveau, Eur. Phys. J. B **15**, 657 (2000).
[13] Y. B. Kudasov, Phys. Rev. Lett. **96**, 027212 (2006).
[14] U. K. Rößler and A. N. Bogdanov, J. Magn. Magn. Mater. **269**, L287 (2004).
[15] W. Wang, D.-D. Chen, D. Lv, J.-P. Liu, Q. Li, and Z. Peng, J. Phys. Chem. Solids **108**, 39 (2017).
[16] D. Lv, F. Wang, R.-J. Liu, Q. Xue, and S.-X. Li, J. Alloys Comp. **701**, 935 (2017).
[17] T. Kaneyoshi, Phys. Status Solidi B **248**, 250 (2011).
[18] R. Masrour, A. Jabar, A. Benyoussef, M. Hamedoun, and L. Bahmad, Physica B (Amsterdam) **472**, 19 (2015).
[19] J. Ahmed, S. Sharma, K. V. Ramanujachary, S. E. Lofland, and A. K. Ganguli, J. Colloid Interface Sci. **336**, 814 (2009).
[20] Y.-B. Chen, L. Chen, and L.-M. Wu, Crystal Growth Design **8**, 2736 (2008).
[21] D. Wood and H. Griffiths, J. Phys. C **5**, L253 (1972).
[22] R. J. Baxter and F. Wu, Phys. Rev. Lett. **31**, 1294 (1973).
[23] R. Baxter, Aust. J. Phys. **27**, 369 (1974).
[24] R. Baxter and F. Wu, Aust. J. Phys. **27**, 357 (1974).
[25] N. W. Ashcroft and D. N. Mermin, in *Solid State Physics*, edited by D. G. Crane (Saunders College Publishing, Philadelphia, 1976), p. 69.
[26] L. N. Jorge, L. S. Ferreira, S. A. Leão, and A. A. Caparica, Braz. J. Phys. **46**, 556 (2016).
[27] M. Santos and W. Figueiredo, Phys. Rev. E **63**, 042101 (2001).
[28] I. Velonakis and S. Martinos, Physica A (Amsterdam) **392**, 2016 (2013).
[29] F. Wang and D. P. Landau, Phys. Rev. E **64**, 056101 (2001).
[30] A. A. Caparica and A. G. Cunha-Netto, Phys. Rev. E **85**, 046702 (2012).
[31] A. A. Caparica, Phys. Rev. E **89**, 043301 (2014).
[32] L. Ferreira, L. Jorge, S. Leão, and A. Caparica, J. Comput. Phys. **358**, 130 (2018).
[33] K. Binder, Rep. Prog. Phys. **60**, 487 (1997).
[34] M. E. Fisher and A. N. Berker, Phys. Rev. B **26**, 2507 (1982).
[35] J. Lee and J. M. Kosterlitz, Phys. Rev. B **43**, 3265 (1991).
[36] A. M. Ferrenberg and D. P. Landau, Phys. Rev. B **44**, 5081 (1991).

[37] A. A. Caparica, A. Bunker, and D. P. Landau, Phys. Rev. B **62**, 9458 (2000).

[38] A. Caparica, S. A. Leão, and C. J. DaSilva, Physica A (Amsterdam) **438**, 447 (2015).

[39] L. D. Roelofs, A. R. Kortan, T. L. Einstein, and R. L. Park, Phys. Rev. Lett. **46**, 1465 (1981).

[40] P. Piercy and H. Pfnür, Phys. Rev. Lett. **59**, 1124 (1987).

[41] L. Schwenger, K. Budde, C. Voges, and H. Pfnür, Phys. Rev. Lett. **73**, 296 (1994).

[42] G. T. Barkema, M. E. J. Newman, and M. Breeman, Phys. Rev. B **50**, 7946 (1994).